# CHAPTER 2

# TRANSPORT MODEL

## 2.1 PERMEABILITY-SOLUBILITY-CHARGE STATE AND THE pH PARTITION HYPOTHESIS

Fick's first law applied to a membrane [18,40–42] shows that passive diffusion of a solute is the product of the diffusivity and the concentration gradient of the solute *inside* the membrane. The membrane/water apparent partition coefficient relates the latter internal gradient to the external bulk water concentration difference between the two solutions separated by the membrane. For an ionizable molecule to permeate by passive diffusion most efficiently, the molecule needs to be in its uncharged form at the membrane surface. This is the essence of the pH partition hypothesis [44]. The amount of the uncharged form present at a given pH, which directly contributes to the flux, depends on several important factors, such as pH, binding to indigenous carriers (proteins and bile acids), self-binding (aggregate or micelle formation), and solubility (a solid-state form of self-binding). Low solubility enters the transport consideration as a thermodynamic ''speed attenuator,'' as a condition that lowers the opportunity for transport. In this way, permeability and solubility are the linked kinetic and thermodynamic parts of transport across a membrane.

Consider a vessel divided into two chambers, separated by a homogeneous lipid membrane. Figure 2.1 is a cartoon of such an arrangement. The left side is the donor compartment, where the sample molecules are first introduced; the right side is the acceptor compartment, which at the start has no sample molecules.

*Absorption and Drug Development: Solubility, Permeability, and Charge State*. By Alex Avdeef
ISBN 0-471-423653. 

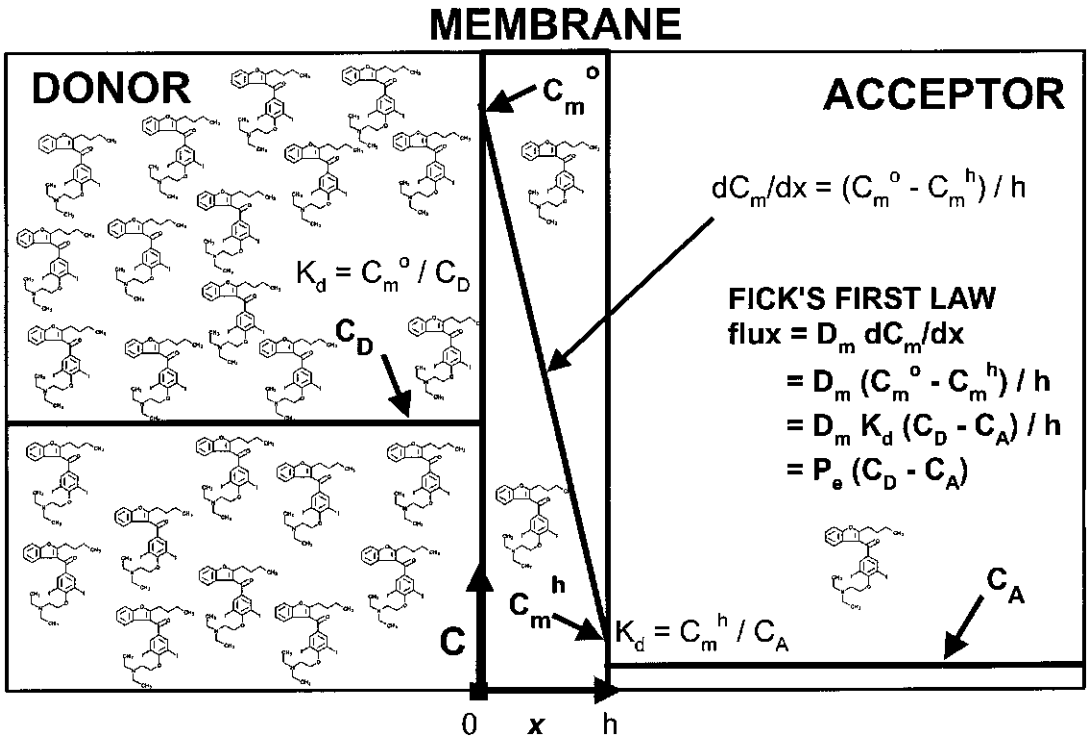


**Figure 2.1** Transport model diagram, depicting two aqueous cells separated by a membrane barrier. The drug molecules are introduced in the donor cell. The concentration gradient in the membrane drives the molecules in the direction of the acceptor compartment. The apparent partition coefficient, $K_d = 2$. [Avdeef, A., *Curr. Topics Med. Chem.*, **1**, 277–351 (2001). Reproduced with permission from Bentham Science Publishers, Ltd.]

Fick's first law applied to homogeneous membranes at steady state is a transport equation

$$J = \frac{D_m dC_m}{dx} = \frac{D_m[C_m^0 - C_m^h]}{h} \tag{2.1}$$

where $J$ is the flux, in units of mol $cm^{-2}$ $s^{-1}$, where $C_m^0$ and $C_m^h$ are the concentrations, in mol/$cm^3$ units, of the *uncharged* form of the solute within the membrane at the two water–membrane boundaries (at positions $x = 0$ and $x = h$ in Fig. 2.1, where $h$ is the thickness of the membrane in centimeters) and where $D_m$ is the diffusivity of the solute within the *membrane*, in units of $cm^2$/s. At steady state, the concentration gradient, $dC_m/dx$, within the membrane is linear, so the difference may be used in the right side of Eq. (2.1). Steady state takes about 3 min to be established in a membrane of thickness 125 μm [19,20], assuming that the solution is very well stirred.

The limitation of Eq. (2.1) is that measurement of concentrations of solute within different parts of the membrane is very inconvenient. However, since we can estimate (or possibly measure) the distribution coefficients between bulk water and the membrane, log $K_d$ (the pH-dependent apparent partition coefficient), we can convert Eq. (2.1) into a more accessible form

$$J = \frac{D_m K_d (C_D - C_A)}{h} \tag{2.2}$$

where the substitution of $K_d$ allows us to use bulk water concentrations in the donor and acceptor compartments, $C_D$ and $C_A$, respectively. (With ionizable molecules, $C_A$ and $C_D$ refer to the concentrations of the solute summed over all forms of charge state.) These concentrations may be readily measured by standard techniques. Equation (2.2) is still not sufficiently convenient, since we need to estimate $D_m$ and $K_d$. It is common practice to lump these parameters and the thickness of the membrane into a composite parameter, called *membrane permeability* $P_m$:

$$P_m = \frac{D_m K_d}{h} \tag{2.3}$$

The relevance of Eq. (2.2) (which predicts how quickly molecules pass through simple membranes) to solubility comes in the concentration terms. Consider "sink" conditions, where $C_A$ is essentially zero. Equation (2.2) reduces to the following flux equation

$$J = P_m C_D \tag{2.4}$$

Flux depends on the product of membrane permeability of the solute times the concentration of the solute (summed over all charge state forms) at the water side of the donor surface of the membrane. This concentration ideally may be equal to the dose of the drug, unless the dose exceeds the solubility limit at the pH considered, in

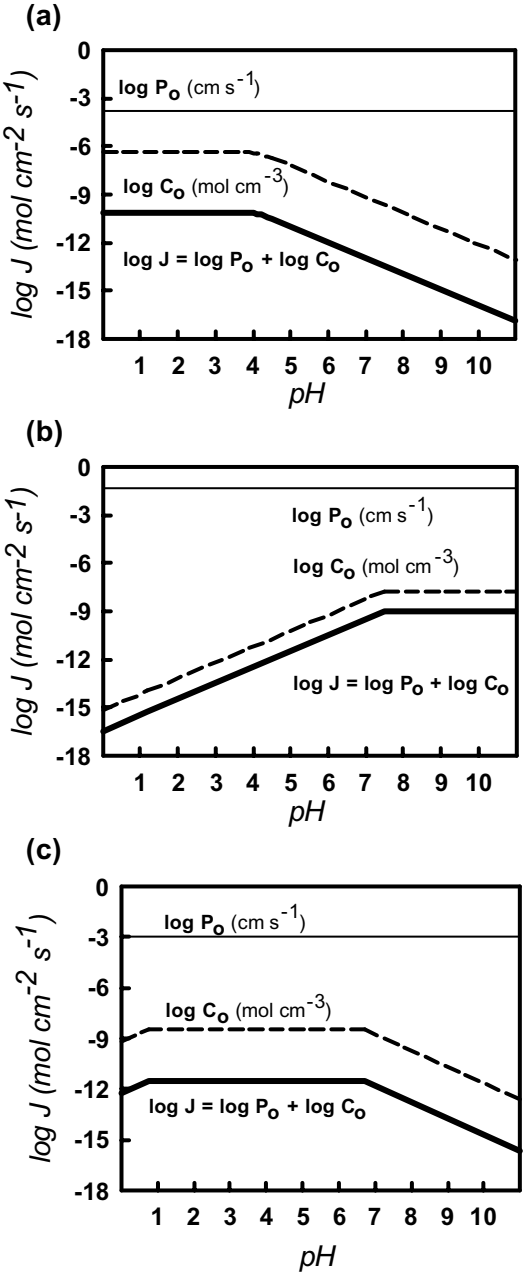


**Figure 2.2** Log flux–pH profiles at dosing concentrations: (a) ketoprofen (acid, p$K_a$ 3.98), dose 75 mg; (b) verapamil (base, p$K_a$ 9.07), dose 180 mg; (c) piroxicam (ampholyte, p$K_a$ 5.07, 2.33), dose 20 mg. The permeability and the concentration of the uncharged species are denoted $P_0$ and $C_0$, respectively. [Avdeef, A., *Curr. Topics Med. Chem.*, **1**, 277–351 (2001). Reproduced with permission from Bentham Science Publishers, Ltd.]

which case it is equal to the solubility. Since the uncharged molecular species is the permeant, Eq. (2.4) may be restated as

$$J = P_0 C_0 \leq P_0 S_0 \tag{2.5}$$

where $P_0$ and $C_0$ are the intrinsic permeability and concentration of the uncharged species, respectively. The intrinsic permeability does not depend on pH, but its cofactor in the flux equation $C_0$ does. The concentration of the uncharged species is always equal to or less than the intrinsic solubility of the specie, $S_0$, which never depends on pH. Note that for the uncharged species, Eq. (2.3) takes on the form

$$P_0 = \frac{D_m K_p}{h} \tag{2.6}$$

where $K_p = C_m(0)/C_{D0}$; also, $K_p = C_m(h)/C_{A0}$; $C_{D0}$ and $C_{A0}$ are the aqueous solution concentrations of the *uncharged* species in the donor and acceptor sides, respectively.

In solutions saturated (i.e., excess solid present) at some pH, the plot of log $C_0$ versus pH for an ionizable molecule is extraordinarily simple in form; it is a combination of straight segments, joined at points of discontinuity indicating the boundary between the saturated state and the state of complete dissolution. The pH of these junction points is dependent on the dose used in the calculation, and the maximum value of log $C_0$ is always equal to log $S_0$ in a saturated solution. [26] Figure 2.2 illustrates this idea using ketoprofen as an example of an acid, verapamil as a base, and piroxicam as an ampholyte. In the three cases, the assumed concentrations in the calculation were set to the respective doses [26]. For an acid, log $C_0$ (dashed curve in Fig. 2.2a) is a horizontal line (log $C_0$ = log $S_0$) in the saturated solution (at low pH), and decreases with a slope of $-1$ in the pH domain where the solute is dissolved completely. For a base (Fig. 2.2b) the plot of log $C_0$ versus pH is also a horizontal line at high pH in a saturated solution and is a line with a slope of $+1$ for pH values less than the pH of the onset of precipitation.

We have called the plot of log $C_0$ versus pH the ''flux factor'' profile, with the idea that such a plot when combined with intrinsic permeability, can be the basis of an in vitro classification scheme to predict passive oral absorption as a function of pH. This will be discussed later.

Figures 2.1 and 2.2 represent the basic model that will be used to discuss the literature related to the measurement of the physicochemical parameters and the interpretation of their role in the oral absorption process [19,20,23,45–61].

## 2.2 PROPERTIES OF THE GASTROINTESTINAL TRACT (GIT)

The properties of the human GIT that are relevant to the absorption of drug products have been collected from several sources [62–69]. Figure 2.3 shows a cartoon of the GIT, indicating surface area and pH (fasted and fed state) in the various

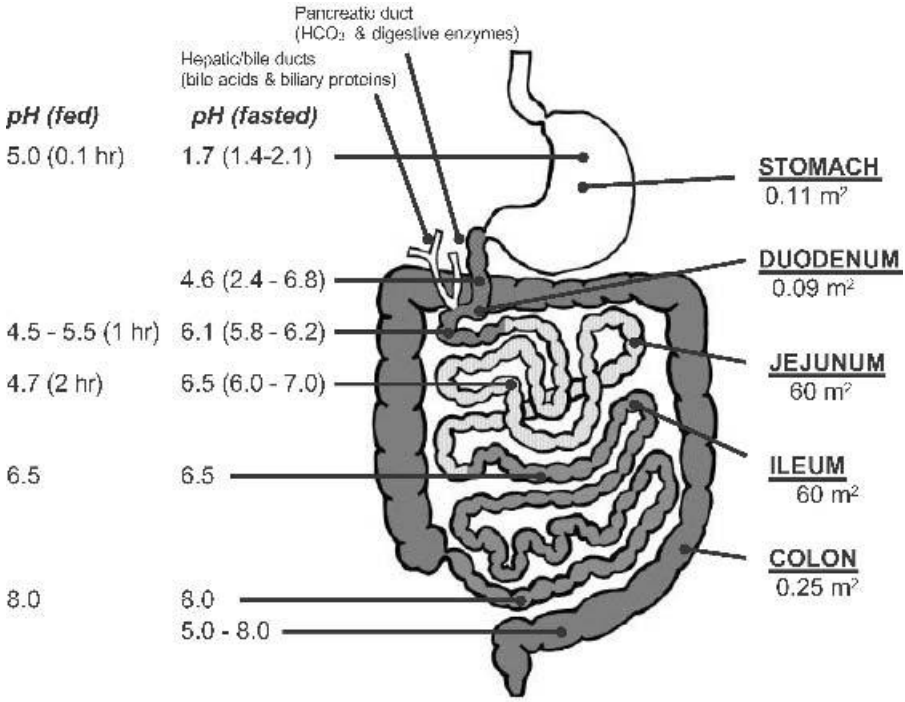


**Figure 2.3** Physical properties of the GIT, with approximate values compiled from several sources [62–69]. The pH values refer mostly to median quantities and the range in parentheses generally refers to interquartile values [67,68]. The quoted surface areas are taken from Ref. 66. [Avdeef, A., *Curr. Topics Med. Chem.*, **1**, 277–351 (2001). Reproduced with permission from Bentham Science Publishers, Ltd.]

segments. The surface area available for absorption is highest in the jejunum and the ileum, accounting for more than 99% of the total. In the fasted state, the pH in the stomach is ∼1.7. The acidified contents of the stomach are neutralized in the duodenum by the infusion of bicarbonate ions through the pancreatic duct. Past the pyloric sphincter separating the stomach and the duodenum, the pH steeply rises to ∼4.6. Between the proximal jejunum and the distal ileum, the pH gradually rises from ∼6 to 8. The pH can drop to values as low as 5 in the colon, due to the microbial digestion of certain carbohydrates, producing short-chain fatty acids (SCFAs) in concentration as high as 60–120 mM. [70] The GIT exhibits a considerable pH gradient, and the pH partition hypothesis predicts that the absorption of ionizable drugs may be location-specific.

When food is ingested, the pH in the stomach can rise briefly to 7, but after 0.1 h drops to pH 5, after 1 h to pH 3, and after 3 h to the fasted value. The movement of food down the small intestine causes the pH in the proximal jejunum to drop to as low as 4.5 in 1–2 h after food intake, but the distal portions of the small intestine and the colon are not dramatically changed in pH due to the transit of food. The

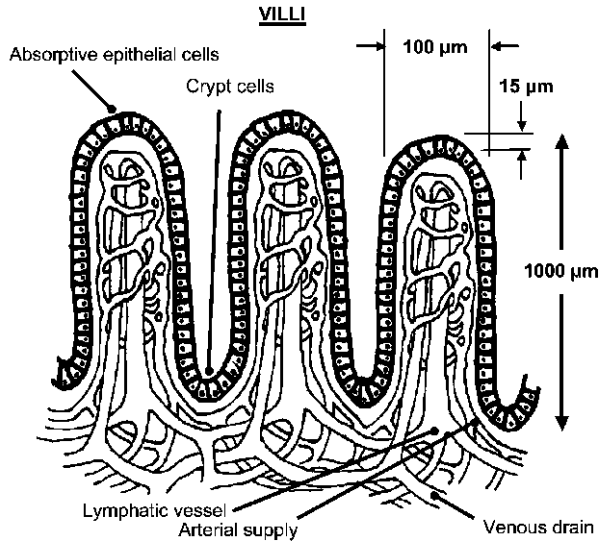


**Figure 2.4** Schematic of the villi "fingers" covered by a monolayer of epithelial cells, separating the lumen from the blood capillary network [63,69]. [Avdeef, A., *Curr. Topics Med. Chem.*, **1**, 277–351 (2001). Reproduced with permission from Bentham Science Publishers, Ltd.]

stomach releases its contents periodically, and the rate depends on the contents. On an empty stomach, 200 mL of water have a transit half-life of 0.1–0.4 h, but solids (such as tablets) may reside for 0.5–3 h, with larger particles held back the longest. Food is retained for 0.5–13 h; fatty food and large particles are held the longest time. Transit time through the jejunum and ileum is about 3–5 h. Digesting food may stay in the colon for 7–20 h, depending on the sleep phase. Fatty foods trigger the release of bile acids, phospholipids, and biliary proteins via the hepatic/bile ducts into the duodenum. Bile acids and lecithin combine to form mixed micelles, which help solubilize lipid molecules, such as cholesterol (or highly lipophilic drugs). Under fasted conditions, the bile : lecithin concentrations in the small intestine are approximately 4 : 1 mM, but a fatty meal can raise the level to about 15 : 4 mM [68,71]. Thus, maximal absorption of drug products takes place in the jejunum and ileum over a period of 3–5 h, in a pH range of 4.5–8.0. This suggests that weak acids ought to be better absorbed in the jejunum, and weak bases in the ileum.

The surface area in the luminal side of the small intestine per unit length of the serosal (blood) side is enormous in the proximal jejunum, and steadily decreases (to about 20% of the starting value [62]) in the distal portions of the small intestine. The surface area is increased threefold [69] by ridges oriented circumferentially around the lumen. Similar folds are found in all segments of the GIT, except the mouth and esophagus [66]. Further 4–10-fold expansion [62,69] of the surface is produced by the villi structures, shown schematically in Fig. 2.4. The layer of epithelial cells lining the villi structures separate the lumen from the circulatory system. Epithelial cells are made in the crypt folds of the villi, and take about

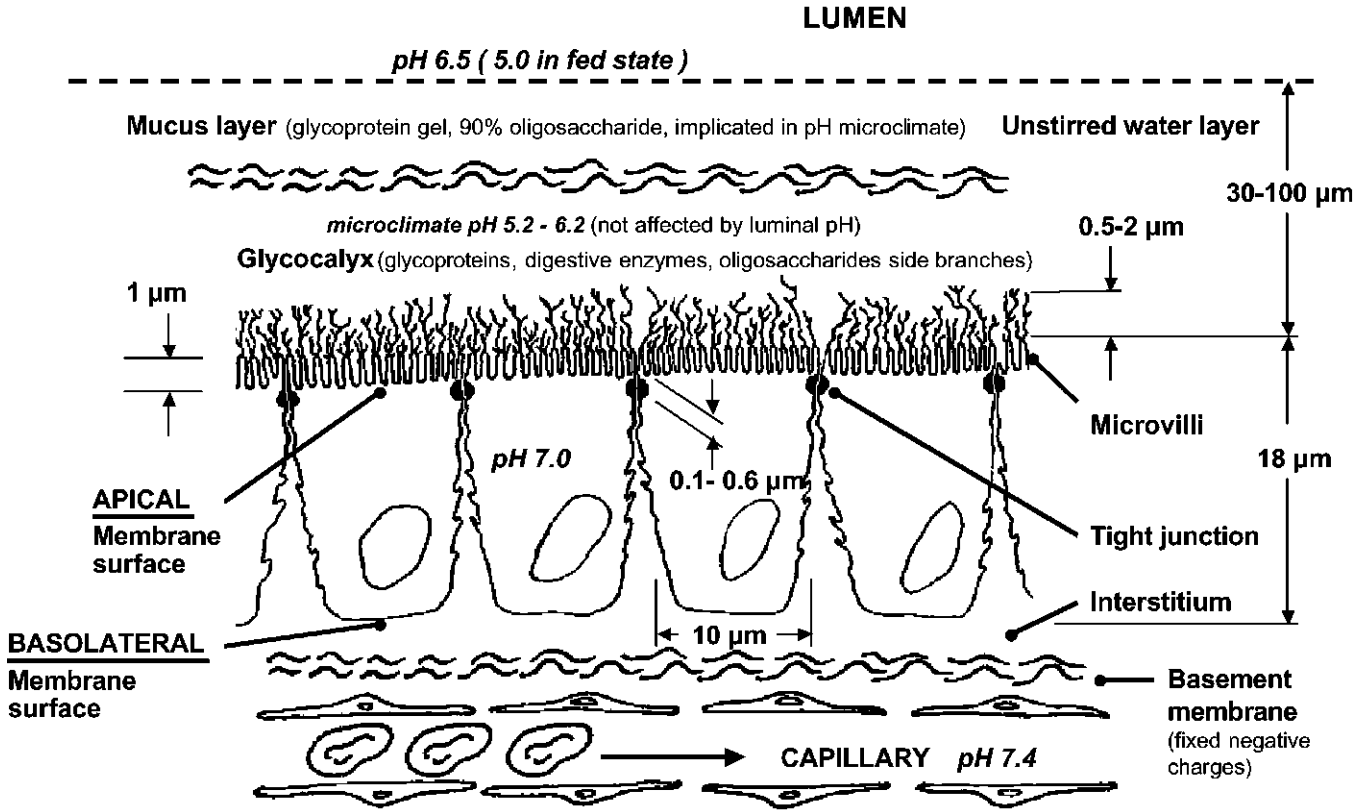


**Figure 2.5** Schematic of the structure of epithelial cells, based on several literature sources [55,63,69,73,74,76,78,79]. The tight junctions and the basement membrane appear to be slightly ion-selective (lined with some negatively charged groups) [75,76,79]. [Avdeef, A., *Curr. Topics Med. Chem.*, **1**, 277–351 (2001). Reproduced with permission from Bentham Science Publishers, Ltd.]

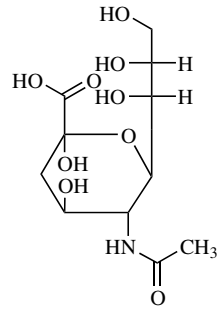


**Figure 2.6** Sialic acid.

2 days to move to the region of the tips of the villi, where they are then shed into the lumen. A schematic view of the surface of the epithelial cells shows a further 10–30-fold surface expansion [62,63,69] structures, in the form of microvilli on the luminal side of the cell layer, as shown in Fig. 2.5.

The villi and microvilli structures are found in highest density in the duodenum, jejunum, and ileum, and in lower density in a short section of the proximal colon [66]. The microvilli have glycoproteins (the glycocalyx) protruding into the luminal fluid. There is residual negative charge in the glycoproteins. Some cells in the monolayer are known as goblet cells (not shown in Figs. 2.4 and 2.5), whose function is to produce the mucus layer that blankets the glycocalyx. The mucus layer is composed of a high-molecular-weight (HMW) ($2 \times 10^6$ Da) glycoprotein, which is 90% oligosaccharide, rich in sialic acid (Fig. 2.6) residues, imparting negative charge to the layer [63]. Studies of the diffusion of drug molecules through the mucus layer suggest that lipophilic molecules are slowed by it [72].

The glycocalyx and the mucus layer make up the structure of the unstirred water layer (UWL) [73]. The thickness of the UWL is estimated to be 30–100 μm in vivo, consistent with very efficient stirring effects [74]. In isolated tissue (in the absence of stirring), the mucus layer is 300–700 μm thick [73]. The pH in the unstirred water layer is ~5.2–6.2, and might be regulated independently of the luminal pH (Section 2.3). The mucus layer may play a role in regulating the epithelial cell surface pH [73].

The membrane surface facing the lumen is called the *apical surface*, and the membrane surface on the side facing blood is called the *basolateral surface*. The intestinal cells are joined at the tight junctions [63,75]. These junctions have pores that can allow small molecules (MW < 200 Da) to diffuse through in aqueous solution. In the jejunum, the pores are ~7–9 Å in size. In the ileum the junctions are tighter, and pores are ~3–4 Å in size (i.e., dimensions of mannitol) [63].

The apical surface is loaded with more than 20 different digestive enzymes and proteins; the protein : lipid ratio is high: 1.7 : 1 [63]. The half-life of these proteins is ~6–12 h, whereas the epithelial cells last 2–3 days. So the cell must replace these constituents without depolarizing itself. The cytoskeleton may play a role

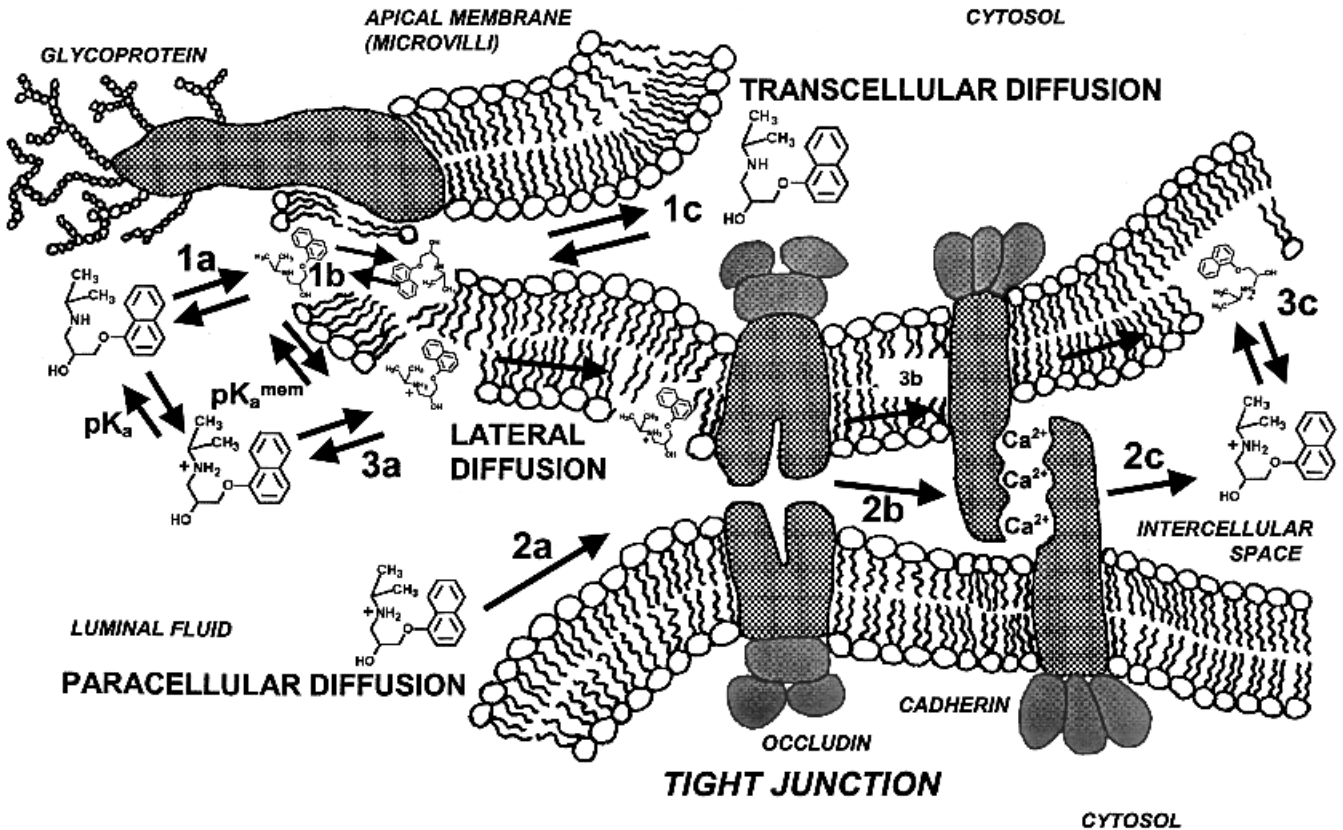


**Figure 2.7** Schematic of the apical phospholipid bilayer surface of the epithelial cells, indicating three types of passive diffusion: transcellular (1a→1b→1c), paracellular (2a→2b→2c), and the hypothesized lateral, ''under the skin of the tight junction'' (3a→3b→3c) modes. Tight-junction matrix of proteins highly stylized, based on Ref. 75. [Avdeef, A., *Curr. Topics Med. Chem.*, **1**, 277–351 (2001). Reproduced with permission from Bentham Science Publishers, Ltd.]

in maintaining the polar distribution of the surface constituents [63]. After a permeant passes through the cell barrier, it encounters a charge-selective barrier in the basement membrane (Fig. 2.5) [76]. Positively charged drugs have a slightly higher permeability through it. After this barrier, drug molecules may enter the blood capillary network through openings in the highly fenestrated capillaries. Epithelial cell surfaces are composed of bilayers made with phospholipids, as shown in the highly stylized drawing in Fig. 2.7.

Two principal routes of passive diffusion are recognized: transcellular (1a → 1b → 1c in Fig. 2.7) and paracellular (2a → 2b → 2c). Lateral exchange of phospholipid components of the *inner* leaflet of the epithelial bilayer seems possible, mixing simple lipids between the apical and basolateral side. However, whether the membrane lipids in the *outer* leaflet can diffuse across the tight junction is a point of controversy, and there may be some evidence in favor of it (for some lipids) [63]. In this book, a third passive mechanism, based on lateral diffusion of drug molecules in the outer leaflet of the bilayer (3a → 3b → 3c), will be hypothesized as a possible mode of transport for polar or charged amphiphilic molecules.

In the transport across a phospholipid bilayer by passive diffusion, the permeability of the neutral form of a molecule is $\sim 10^8$ times greater than that of the charged form. For the epithelium, the discrimination factor is $10^5$. The basement membrane (Fig. 2.5) allows passage of uncharged molecules more readily than charged species by a factor of 10 [76].

## 2.3 pH MICROCLIMATE

The absorption of short-chain weak acids in the rat intestine, as a function of pH, does not appear to conform to the pH partition hypothesis [44]. Similar anomalies were found with weak bases [77]. The apparent p$K_a$ values observed in the absorption–pH curve were shifted to higher values for acids and to lower values for bases, compared with the true p$K_a$ values. Such deviations could be explained by the effect of an acid layer on the apical side of cells, the so-called acid pH microclimate [44,70,73,76–84].

Shiau et al. [73] directly measured the microclimate pH, $pH_m$, to be 5.2–6.7 in different sections of the intestine (very reproducible values in a given segment) covered with the normal mucus layer, as the luminal (bulk) pH, $pH_b$, was maintained at 7.2. Good controls ruled out pH electrode artifacts. With the mucus layer washed off, $pH_m$ rose from 5.4 to 7.2. Values of $pH_b$ as low as 3 and as high as 10 remarkably did not affect values of $pH_m$. Glucose did not affect $pH_m$ when the microclimate was established. However, when the mucus layer had been washed off and $pH_m$ was allowed to rise to $pH_b$, the addition of 28 mM glucose caused the original low $pH_m$ to be reestablished after 5 min. Shiau et al. [73] hypothesized that the mucus layer was an ampholyte (of considerable pH buffer capacity) that created the pH acid microclimate.

Said et al. [78] measured $pH_m$ in rat intestine under in vitro and in vivo conditions. As $pH_b$ was kept constant at 7.4, $pH_m$ values varied within 6.4–6.3 (proximal

to distal duodenum), 6.0–6.4 (proximal to distal jejunum), 6.6–6.9 (proximal to distal ileum), and were 6.9 in the colon. Serosal surface had normal pH. When glucose or sodium was removed from the bathing solutions, the $pH_m$ values began to rise. Metabolic inhibitors (1 mM iodoacetate or 2,4-dinitrophenol) also caused the $pH_m$ values to rise. Said et al. [78] hypothesized that a $Na^+/H^+$ antiporter mechanism, dependent on cellular metabolism, was responsible for the acid pH microclimate.

The tips of villi have the lowest $pH_m$ values, whereas the crypt regions have $pH_m > 8$ values [70]. Most remarkable was that an alkaline microclimate ($pH_m$ 8) was observed in the human stomach, whose bulk $pH_b$ is generally about 1.7. In the stomach and duodenum, the near-neutral microclimate pH was attributed to the secretion of $HCO_3^-$ from the epithelium [70].

## 2.4 INTRACELLULAR pH ENVIRONMENT

Asokan and Cho [83] reviewed the distribution of pH environments in the cell. Much of what is known in the physiological literature was determined using pH-sensitive fluorescent molecules and specific functional inhibitors. The physiological pH in the cytosol is maintained by plasma membrane-bound $H^+$-ATPases, ion exchangers, as well as the $Na^+/K^+$-APTase pumps. Inside the organelles, pH microenvironments are maintained by a balance between ion pumps, leaks, and internal ionic equilibria. Table 2.1 lists the approximate pH values of the various cellular compartments.

## 2.5 TIGHT-JUNCTION COMPLEX

Many structural components of the tight junctions (TJs) have been defined since 1992 [85–97]. Lutz and Siahaan [95] reviewed the protein structural components of the TJ. Figure 2.7 depicts the occludin protein complex that makes the water pores so restrictive. Freeze-fracture electronmicrographs of the constrictive region of the TJ show net-like arrays of strands (made partly of the cytoskeleton) circumscribing the cell, forming a division between the apical and the basolateral

**TABLE 2.1 Intracellular pH Environment**

| Intracellular Compartment | pH |
|---|---|
| Mitocondria | 8.0 |
| Cytosol | 7.2–7.4 |
| Endoplasmic reticulum | 7.1–7.2 |
| Golgi | 6.2–7.0 |
| Endosomes | 5.5–6.0 |
| Secretory granules | 5.0–6.0 |
| Lysosomes | 4.5–5.0 |

*Source:* Ref. 83.

sides. A region 10 strands wide forms junctions that have very small pore openings; fewer strands produce leakier junctions. The actual cell-cell adhesions occur in the cadheren junctions, located further away from the apical side. Apparently three calciums contiguously link 10-residue portions of cadheren proteins spanning from two adjoining cell walls, as depicted in Fig. 2.7 [95]. Calcium-binding agents can open the junctions by interactions with the cadheren complex.

## 2.6 STRUCTURE OF OCTANOL

Given the complexities of the phospholipid bilayer barriers separating the luminal contents from the serosal side, it is remarkable that a simple 'isotropic' solvent system like octanol has served so robustly as a model system for predicting transport properties [98]. However, most recent investigations of the structure of water-saturated octanol suggest considerable complexity, as depicted in Fig. 2.8 [99,100]. The 25 mol% water dissolved in octanol is not uniformly dispersed. Water clusters form, surrounded by about 16 octanols, with the polar hydroxyl groups pointing to the clusters and intertwined in a hydrogen-bonded network.

The aliphatic tails form a hydrocarbon region with properties not too different from the hydrocarbon core of bilayers. The clusters have an interfacial zone

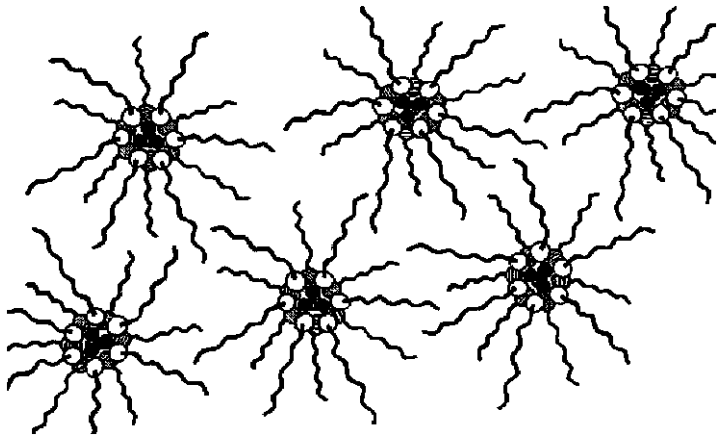

**Figure 2.8** Modern structure of wet octanol, based on a low-angle X-ray diffraction study [100]. The four black circles at the center of each cluster represent water molecules. The four hydrogen-bonded water molecules are in turn surrounded by about 16 octanol molecules (only 12 are shown), H-bonded mutually and to the water molecules. The aliphatic tails of the octanol molecules form a hydrocarbon region largely free of water molecules. It is thought that ion-paired drug molecules are located in the water–octanol clusters, and thus can readily diffuse through the ''isotropic'' medium. For example, filters impregnated with octanol show substantial permeability of charged drug species. However, permeabilities of charged drugs in filters impregnated with phospholipid–alkane solutions are extremely low. [Avdeef, A., *Curr. Topics Med. Chem.*, **1**, 277–351 (2001). Reproduced with permission from Bentham Science Publishers, Ltd.]

between the water interior and the octanol hydroxyl groups. Since water can enter octanol, charged drug molecules need not shed their solvation shells upon entry into the octanol phase. Charged drugs, paired up with counterions (to maintain charge neutrality in the low dielectric medium of octanol, $\epsilon = 8$), can readily diffuse in octanol. Phospholipid bilayers may not have a comparable mechanism accorded to charged lipophilic species, and free diffusion may not be realizable.

## 2.7 BIOPHARMACEUTICS CLASSIFICATION SYSTEM

The transport model considered in this book, based on permeability and solubility, is also found in the biopharmaceutics classification system (BCS) proposed by the U.S. Food and Drug Administration (FDA) as a bioavailability–bioequivalence (BA/BE) regulatory guideline [101–110]. The BCS allows estimation of the likely contributions of three major factors—dissolution, solubility, and intestinal permeability—which affect oral drug absorption from immediate-release solid oral products. Figure 2.9 shows the four BCS classes, based on high and low designations of solubility and permeability. The draft document posted on the FDA website details the methods for determining the classifications [106]. If a molecule is classed as highly soluble, highly permeable (class 1), and does not have a narrow therapeutic index, it may qualify for a waiver of the very expensive BA/BE clinical testing.

The solubility scale is defined in terms of the volume (mL) of water required to dissolve the highest dose strength at the lowest solubility in the pH 1–8 range, with 250 mL as the dividing line between high and low. So, high solubility refers to complete dissolution of the highest dose in 250 mL in the pH range 1–8. Permeability is the major rate-controlling step when absorption kinetics from the GIT is controlled

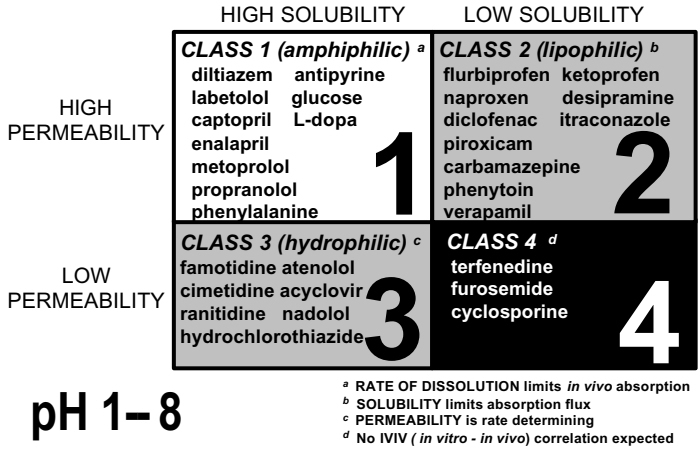


**Figure 2.9** Biopharmaceutics classification system [101–110]. Examples are from Refs. 102 and 104. [Avdeef, A., *Curr. Topics Med. Chem.*, **1**, 277–351 (2001). Reproduced with permission from Bentham Science Publishers, Ltd.]

by drug biopharmaceutical factors and not by formulation factors. Extending the BCS to low-permeability drugs would require that permeability and intestinal residence time not be affected by excipients [110].

Permeability in the BCS refers to human jejunal values, where ''high'' is $\geq 10^{-4}$ cm/s and ''low'' is below that value. Values of well-known drugs have been determined in vivo at pH 6.5 [56]. The high permeability class boundary is intended to identify drugs that exhibit nearly complete absorption (>90% of an administered oral dose) from the small intestine. The class boundary is based on mass balance determination or in comparison to an intravenous reference dose, without evidence suggesting instability in the gastrointestinal tract. Intestinal membrane permeability may be measured by in vitro or in vivo methods that can predict extent of drug absorption in humans. It is curious that so little emphasis is placed on the pH dependence of permeability assessment, given that the small intestine is a pH gradient spanning about 5–8.

The rapid dissolution class boundary is defined in terms of the in vitro dissolution being greater than 85% in 30 min in 900 mL aqueous media at pH 1, 4.5, and 6.8, using USP Apparatus I (100 rpm) or Apparatus II [50 rpm (revolutions/min)] [104]. A similar guideline has been introduced in the European Union [105]. Examples of molecules from the various four classes are presented in Fig. 2.9 [102,104].